Equilibrium Structure and Stability of AlC_n (n = 2, 3) and AlC_nN (n = 1, 2) Species

Xiang'e Zheng, Zhizhong Wang,* and Auchin Tang

Institute of Theoretical Chemistry, State Key Laboratory of Theoretical and Computational Chemistry, Jilin University, Changchun, 130023, P. R. China

Received: February 16, 1999; In Final Form: July 20, 1999

Stable isomers of AlC_2, AlC_3, AlCN, and AlC_2N and transition states for AlC_2 and AlCN molecules were determined at B3LYP and MP2 levels, and stable isomers of AlC_2 and AlCN (and AlNC) were also calculated with the QCISD method. Vibrational frequencies were calculated to define whether the optimized geometry is a true minimum (for stable isomer) or the first-order saddle point (for transition state). These species were calculated to be primarily ionic bonding toward the Al−C bond and thermodynamically stable. To confirm that the transition states of AlC_2 and AlCN molecules connect the correct stationary points, IRC calculations were performed at the B3LYP and MP2 levels.

1. Introduction

Metallurgic properties of metal carbides have received some attention. Although refractory in the solid state, they may exist in the gas state as astrophysical objects. Some molecules have been investigated[1] by analyzing the unidentified microwave lines taken by a radiotelescope. The carbon star IRC+10216 typically ejects several molecules containing carbon, including MgNC.[2,3] The MgNC molecule has been observed as an interstellar molecule by Kawaguchi et al.[4] and Ishii et al.[5] Ever since then, metal carbides are the subject of considerable interest. Since C is the most abundant organic element in interstellar space and since elements Al and N are also quite abundant in stellar atmosphere, compounds composed of elements C, N, and Al may exist in the gas phase as astrophysical objects, although they have not been observed. There have been theoretical investigations on the characteristics of MgC and MgC_2,[6−10] AlCN, AlNC, and AlC_2[10−15] molecules.

In this work, we performed accurate equilibrium structures and vibrational frequency calculations on all possible forms of AlC_n (n = 2, 3) and AlC_nN (n = 1, 2) molecules. For the two series, we considered both doublet and quadruplet states for AlC_n (n = 2, 3) molecules, and both singlet and triplet states for AlC_nN (n = 1, 2) compounds. With the exception that AlC_3 molecule adopts a quadruplet with C_{2v} symmetry as its ground state, the ground states of all the other molecules are all doublets (AlC_2) or singlets (AlCN, AlNC, and AlC_2N). Since there is no experimental information on these species, it is necessary to determine accurate molecule structure and thermodynamic stability by more reliable methods that consider the effect of electron correlation. The Møller−Plesset perturbation theory MP2 and density functional theory B3LYP methods were applied to our calculations. Intrinsic reaction coordinate (IRC) calculations were performed on AlC_2 and AlNC molecules to confirm that the transition states connect the right two stationary points. It is necessary to calculate the relative energy of each isomer of the series we considered at more accurate levels. Considering the feasibility and necessity, single-point energies of AlC_2 and AlNC (also AlCN) molecules were calculated with the QCISD(T) method at the QCISD optimized geometries. The results will be useful for exploring and analyzing relative interstellar matters.

2. Computational Details

The geometries of AlC_2, AlC_3, AlCN (also AlNC), and AlC_2N molecules were optimized employing analytical gradients[16] with polarized split-valence three-ζ basis set (6-311G*). Møller−Plesset perturbation theory at second-order MP2,[17] density function theory B3LYP,[18] and QCISD[19] methods were employed to treat electron correlation. For open-shell molecules, the UHF wave functions were projected to pure spectroscopic states (PMP2) to eliminate spin contamination. The fundamental vibrational frequencies, normal coordinates, and zero-point energies (ZPE) were calculated with standard FG matrix methods.[17] For AlC_2 and AlNC molecules, IRC[20,21] calculations were carried out at the B3LYP and MP2 levels. All calculations were performed with the Gaussian 94 program.[22]

3. Results and Discussion

3.1. AlC_2. For the AlC_2 molecule, calculations were performed for both the linear AlCC form and the isosceles triangular (C_{2v}) structure. The isosceles triangular isomer (C_{2v}) was predicted to be 8.77 and 21.39 kcal/mol lower in energy than the linear AlCC form at the B3LYP and MP2 levels, respectively. Since electron correlation is expected to favor the nonlinear structure, it is safe to believe that the global minimum of AlC_2 is the isosceles triangular form (C_{2v}). This supports previous studies of Green[6] and Yang et al.[10] The electronic state of the C_{2v} form we considered is $^2A_1$. Total and relative energies of the two forms are listed in Table 1.

The structure parameters of the isosceles triangular and linear AlCC forms are shown in Figure 1. For the C_{2v} structure, the AlC distance was calculated to be 1.941 and 1.905 Å and the CC distance to be 1.265 and 1.289 Å at the B3LYP and MP2 levels, respectively. When these data are compared with those provided by Yang et al.,[10] which were 1.932 and 1.288 Å for Al−C and C−C bond lengths in the CGTO1 calculation, the difference of the AlC or CC distance is only 0.001−0.03 Å. We also calculated the CC distance in C_2 species and got values

* To whom correspondence should be addressed.

10.1021/jp990569q CCC: $18.00
Published on Web 10/30/1999

TABLE 1: Total Energies and Zero-Point Energies of AlC_n ($n = 2, 3$) and AlC_nN ($n = 1, 2$) at B3LYP/6-311G* and MP2/6-311G* Levels[a]

species	*E*, hartree	*Z*, hartree	*T*, hartree	RE, hartree
AlC_2, **I** (C_{2v})	−318.510 271	0.006 327	−318.503 944	0.00
	−317.809 786	0.006 901	−317.802 885	0.00
	−317.843 626	0.000 000	−317.843 626	0.00[t]
II ($C_{\infty v}$)	−318.495 732	0.005 758	−318.489 974	8.77
	−317.774 540	0.005 744	−317.768 796	21.39
	−317.825 481	0.000 000	−317.825 481	11.39[t]
AlC_3, **I** (C_{2v})	−356.519 818	0.010 793	−356.509 025	0.00
	−355.697 793	0.010 584	−355.687 209	0.00
II ($C_{\infty v}$)	−356.408 557	0.012 011	−356.396 547	70.58
	−355.603 192	0.013 295	−355.589 897	61.06
III ($C_{\infty v}$)	−356.285 045	0.010 680	−356.274 365	147.25
	−355.510 678	0.013 110	−355.497 568	119.00
AlNC ($C_{\infty v}$)	−335.312 686	0.006 510	−335.306 177	0.00
	−334.581 571	0.006 358	−334.575 213	0.00
	−334.617 696	0.000 000	−334.617 696	0.00[t]
AlCN ($C_{\infty v}$)	−335.303 344	0.006 831	−335.296 513	6.06
	−334.579 775	0.006 466	−334.573 309	1.19
	−334.611 254	0.000 000	−334.611 254	4.04[t]
AlC_2N, **I** (C_s)	−373.272 256	0.010 101	−373.262 155	0.00
	−372.428 733	0.010 118	−372.418 615	0.00
II ($C_{\infty v}$)	−373.170 755	0.013 552	−373.157 202	65.86
	−372.345 982	0.012 448	−372.333 534	53.39
III (C_{2v})	−373.128 131	0.008 909	−373.119 222	89.69
	−372.276 927	0.009 314	−372.267 613	94.76
IV ($C_{\infty v}$)	−373.126 952	0.013 097	−373.113 855	93.06
	−372.286 924	0.012 243	−372.274 681	90.32
V ($C_{\infty v}$)	−373.121 172	0.013 047	−373.108 126	96.65
	−372.286 141	0.012 199	−372.273 942	90.78
VI ($C_{\infty v}$)	−373.101 617	0.011 180	−373.090 437	107.75
	−372.261 612	0.010 651	−372.250 961	105.20
VII ($C_{\infty v}$)	−373.094 330	0.010 752	−373.083 577	112.06
	−372.245 027	0.010 581	−372.234 446	115.57
Al	−242.386 073	0.000 000	−242.386 073	
	−241.903 030	0.000 000	−241.903 030	
C_2N (C_{2v})	−130.761 132	0.006 535	−130.754 597	
	−130.436 122	0.006 522	−130.429 600	
C_3 ($D_{\infty h}$)	−114.073 964	0.008 201	−114.065 763	
	−113.728 415	0.008 397	−113.720 018	
C_2 ($D_{\infty h}$)	−75.892 607	0.005 038	- 75.887 570	
	−75.668 794	0.004 748	−75.663 068	
C (^{3}P)	−37.855 989	0.000 000	−37.855 989	
	−37.746 073	0.000 000	−37.746 073	
N (^{2}P)	−54.494 957	0.000 000	−54.494 957	
	−54.349 242	0.000 000	−54.349 242	

[a] For each species, the first and second lines are values for B3LYP and MP2 calculations, respectively. Symbol t represents relative energies at QCISD(T) level. *E*, *Z*, *T* represent electronic energies excluding zero-point energies (ZPE), ZPE, and total energies considering zero-point energies, respectively. RE = relative energy.

TABLE 2: Dissociation and Atomization Energies of AlC_n ($n = 2, 3$) and AlC_nN ($n = 1, 2$) Species

reaction	B3LYP, kcal/mol	MP2, kcal/mol
AlC_2 (**I**,C_{2v}) → Al + C_2	144.52	150.66
AlC_3 (**I**,C_{2v}) → AlC_2 (**I**,C_{2v}) + C	93.56	84.67
AlC_3 (**I**,C_{2v}) → Al + C_3 ($D_{\infty h}$)	35.89	40.26
AlC_2N (**I**,C_s) → AlCN (**I**, $C_{\infty v}$) + C	68.81	62.27
AlC_2N (**I**, C_s) → Al + C_2N (C_{2v})	76.23	53.96
AlC_2N (**I**, C_s) → AlC_2 (**I**,C_{2v}) + N	165.19	165.15

of 1.267 (B3LYP) and 1.285 Å (MP2). We can see that the distance deviation of CC in AlC_2 is much smaller than that in the C_2 species by about 0.004 Å. From this point of view, the electronic structure of AlC_2 can be best described as $Al^+C_2^-$. The normal CC triple bond, double bond, and single bond distances are 1.203, 1.339, and 1.536 Å, respectively. While the bond lengths for C−C are 1.265 (B3LYP) and 1.289 (MP2) Å for the C_{2v} isomer and 1.248 (B3LYP) and 1.262 (MP2) Å for the linear AlCC form, the interactions between two C atoms in AlC_2 should be triple-bonded to some extent. The Mulliken population analyses of the two isomers and charge distribution of the global minimum C_{2v} form are provided in Tables 3 and 4, respectively. The dipole moments in the triangular form were predicted to be 3.99 (B3LYP) and 4.55 (MP2) D. Compared with 4.3, 5.1, and 4.97 D, which were provided by Yang et al.,[10] Flores and Largo,[11] and Knight et al.,[12] respectively, our data are reasonable.

TABLE 3: Population Analysis in AlC_n ($n = 2, 3$) and AlC_nN ($n = 1, 2$) Species at B3LYP Level (with Corresponding Values at MP2 Level in Parentheses)

species	P_{Al-C}	P_{Al-N}	P_{C-C}	P_{C-N}
AlC_2 (**I**, C_{2v})	0.266 (0.294)		0.407 (0.301)	
AlC_3 (**I**, C_{2v})	−0.045 (−0.023)[a]		0.335 (0.243)[c]	
	0.342 (0.321)[b]		−0.097 (−0.102)[d]	
AlNC ($C_{\infty v}$)	0.020 (0.015)	0.154		0.538 (0.503)
AlC_2N (**I**, C_s)	0.108 (0.071)		0.142 (0.059)	0.241 (0.189)[e]
				0.202 (0.181)[f]

[a] For Al−C1. [b] For Al−C2. [c] For C1−C2. [d] For C2−C3. [e] For C1−N. [f] For C2−N bonds.

Fundamental vibrational frequencies in the two forms at both B3LYP and MP2 levels were predicted to be positive. The lowest values are 361.6 (B3LYP) and 578.6 (MP2) cm^{-1} for the C_{2v} form and 85.9 (B3LYP) and 55.8 (MP2) cm^{-1} for the linear one. Thus, we believe that both the two structures are stationary points of AlC_2 molecule. Vibrational frequencies and the corresponding IR intensities are provided in Table 5.

To determine accurate relative energies of the C_{2v} and $C_{\infty v}$ isomers of AlC_2 molecules, the QCISD method, which considers the effect of correlation more completely, was applied to optimize the geometries and calculate the corresponding frequencies. The obtained geometrical parameter and frequencies are given in the brackets in Figure 1 and Table 5, respectively. For the QCISD optimized structures, single-point energies were calculated at the QCISD(T) level, and the C_{2v} isomer was determined to be 11.39 kcal/mol more stable than the $C_{\infty v}$ one.

The isomerization pathway between the lowest C_{2v} and the second low-lying linear $C_{\infty v}$ configuration of AlC_2 was searched with B3LYP and MP2 calculations. The optimized geometries of the transition states are presented in Figure 1. The intrinsic reaction coordinate (IRC) calculation confirms that the obtained transition state connects just the two stationary points of AlC_2, i.e., C_{2v} and $C_{\infty v}$ isomers. The stable C_{2v} isomer can rearrange to the C_s one with a barrier of 8.89 (B3LYP) or 23.59 (MP2) kcal/mol, while the reverse barrier from the $C_{\infty v}$ to C_{2v} isomer is only 0.12 (B3LYP) or 2.20 (MP2) kcal/mol. Obviously, once the linear $C_{\infty v}$ isomer is formed in some circumstance, it will easily convert to the C_{2v} isomer, passing the C_s transition state of AlC_2. Given the energy of the C_{2v} isomer to be 0.00, the relative energy of the $C_{\infty v}$ stable isomer is 8.77, 21.39, and 11.39 kcal/mol at the B3LYP, MP2, and QCISD(T) levels, respectively. In SDCI calculations of Yang et al.[10] and in CASSCF calculations of Chertihin et al.,[13] the C_{2v} isomer is 7 and 8 kcal/mol lower in energy than the $C_{\infty v}$ isomer. Our results at the B3LYP and QCISD(T) levels agree well with those of the above-mentioned studies. The pathway of isomerization of the AlC_2 molecule is plotted in Figure 2.

3.2. AlC_3. There is no previous information on the AlC_3 molecule. We performed calculations on all possible forms and got three true minima at both B3LYP and MP2 levels. The three minima are as follows: the planar C_{2v}, linear AlCCC ($C_{\infty v}$), and the CAlCC forms. In the C_{2v} form, the Al atom bonds with

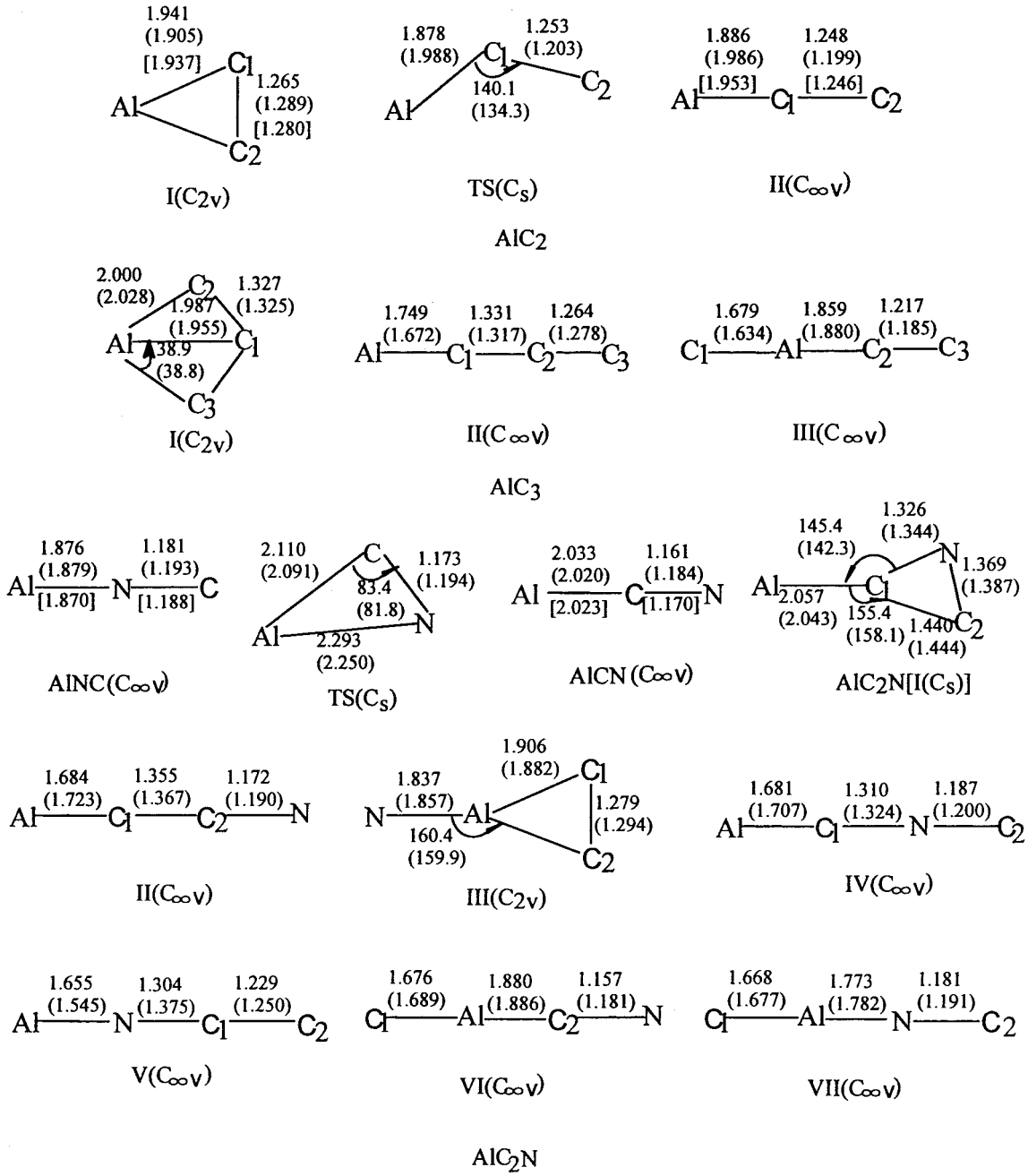

Figure 1. Optimized geometries for AlC_n (n = 2, 3), AlC_nN (n = 1, 2) species and transition states for AlC_2 and AlNC molecules at B3LYP, MP2 (in parentheses), and QCISD (in brackets) levels.

TABLE 4: Charge Distribution on Global Minima of AlC_n (n = 2, 3) and AlC_nN (n = 1, 2) Species

	B3LYP			MP2		
species	Q_{Al}	Q_N	Q_C	Q_{Al}	Q_N	Q_C
AlC_2 (**I**, C_{2v})	0.446		−0.223	0.483		−0.241
AlC_3 (**I**, C_{2v})	0.589		0.033[a]	0.642		0.013[a]
			−0.311[b]			−0.327[b]
AlNC ($C_{\infty v}$)	0.460	−0.445	−0.014	0.506	−0.467	−0.039
AlC_2N (**I**, C_s)	0.433	−0.096	−0.251[a]	0.493	−0.097	−0.303[a]
			−0.086[b]			−0.094[b]

[a] For number one C atom. [b] For number two C atoms.

all three C atoms. On the basis of B3LYP and MP2 calculations, their total energies were predicted to increase along AlC_3 (C_{2v}) → AlCCC → CAlCC. For the C_{2v} structure, the quadruplet is much more stable than the doublet on the basis of our calculations, and its energy is 47.28 (B3LYP) and 14.25 (MP2) kcal/mol lower than that of the doublet state. Provided that the total energy of C_{2v} form is 0.00, the energies of the AlCCC and CAlCC forms were predicted to be 70.58 and 147.25 kcal/mol at the B3LYP level or 61.06 and 119.00 kcal/mol by MP2 calculations. The ground state of AlC_3 was predicted to adopt the $^4B_1$ electronic state. Thus, the $C_{2v}(^4B_1)$ form can be concluded to be the global minimum of the AlC_3 molecule, and this is opposite to that of MgC_3 molecule, for which a similar C_{2v} structure has the highest energy among its three stationary points according to our previous paper.[23]

The structures and optimized geometries of the three forms are given in Figure 1. In the C_{2v} form, one of the three AlC distances is a little shorter than the other two. The shorter Al−C bond length is 1.987 (B3LYP) and 1.955 (MP2) Å, and the longer one for the other two Al−C bonds is 2.000 (B3LYP) and 2.028 (MP2) Å. The distances of the two symmetric CC (C1−C2 and C1−C3 in Figure 1) are 1.327 and 1.325 Å based

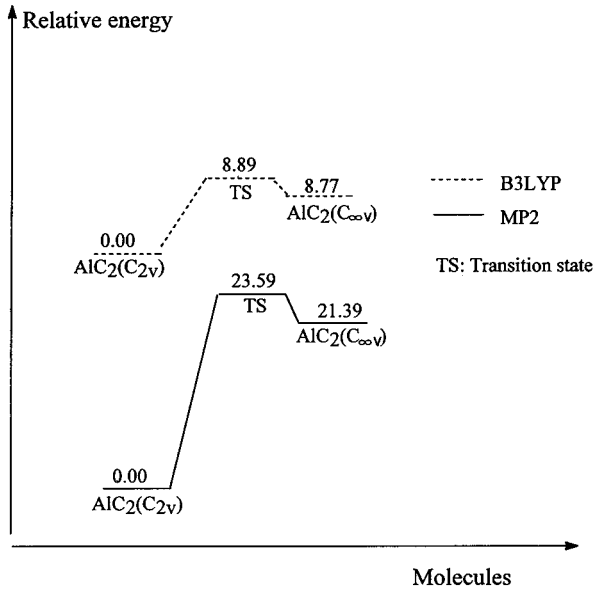

Figure 2. Relative energies of AlC_2 (C_{2v}) and AlC_2 ($C_{\infty v}$) and activation energy of the isomerization between C_{2v} and $C_{\infty v}$ isomers at B3LYP and MP2 levels.

TABLE 5: Calculated Frequencies for Global Minima of AlC_n (n = 2, 3) and AlC_nN (n = 1, 2) Species and Corresponding IR Intensity in Parentheses

species		B3LYP/6-31G*//B3LYP/6-31G*, cm^{-1}	MP2/6-31G*//MP2/6-31G*, cm^{-1}	QCISD/6-311G*//QCISD/6-311G*, cm^{-1}
AlC_2 (**I**, C_{2v})	b_2	361.6 (11)	578.6 (67)	404.8 (17)
	a_1	615.1 (2)	753.4 (83)	624.4
	a_1	1800.5 (7)	1697.2 (1)	1761.3
AlC_3 (**I**, C_{2v})	b_2	402.0 (36)	314.2 (70)	
	a_1	460.2 (9)	513.1 (7)	
	a_1	592.8 (48)	607.7 (47)	
	b_1	666.2 (2)	812.6 (28)	
	a_1	1217.2 (26)	1282.6 (17)	
	b_2	1399.3 (15)	1115.9 (232)	
AlNC ($C_{\infty v}$)	π	102.8 (1)	100.8 (2)	116.1 (1)
	σ	542.1 (179)	544.0 (188)	557.3 (182)
	σ	2109.6 (436)	2045.4 (295)	2094.4 (386)
AlC_2N (**I**, C_s)	a′	111.6 (5)	108.6 (5)	
	a″	189.4 (20)	210.3 (20)	
	a′	392.8 (100)	411.5 (106)	
	a′	996.6 (93)	1020.9 (90)	
	a′	1132.2 (4)	1132.7 (8)	
	a′	1611.0 (60)	1557.4 (97)	

on the two methods, respectively, which shows some triple-bonding interaction between the two C atoms.

According to the bond order for the three forms of the AlC_3 molecule shown in Table 3, strong bonding interactions among the three C atoms are obvious. For example, for the C_{2v} form, the bond orders were predicted to be 0.342 (B3LYP) and 0.321 (MP2) for the two symmetric C1−C2 (or C1−C3) bond. The charge distribution on each atom of the most stable form C_{2v} is given in Table 4.

The dipole moments of the C_{2v} isomer were calculated to be 3.29 and 3.63 D at the B3LYP and MP2 levels, respectively, which agree well with each other.

Vibrational frequency calculations were performed on the optimized geometries for all forms we considered. Table 5 lists results for the $C_{2v}(^4B_1)$ form. For the other two linear forms, i.e., the AlCCC and CAlCC isomers, the lowest fundamental vibrational frequencies were both predicted to adopt π symmetry. The data are 179.6 (B3LYP) and 189.0 (MP2) cm^{-1} for the AlCCC form and 143.5 (B3LYP) and 152.6 (MP2) cm^{-1} for the CAlCC isomer, respectively. We can see that values at the B3LYP and MP2 levels agree well with each other.

3.3. AlCN and AlNC. Calculations were done for both AlCN and AlNC in their singlet and triplet states with the B3LYP, MP2, and QCISD methods. At the three levels, AlNC was predicted to have lower energy than AlCN, which is different from the situation of HCN−HNC. At B3LYP, MP2, and QCISD(T) (at the QCISD optimized geometry) levels, AlNC is 6.09, 1.19, and 4.04 kcal/mol more stable than the AlCN molecule, respectively. The optimized geometries of the two forms are provided in Figure 1. In the AlNC structure, the C−N distance was calculated to be 1.181(B3LYP), 1.193 (MP2), and 1.188 (QCISD) Å, while it is 1.161, 1.184, and 1.170 Å for AlCN. The bond orders for the Al atom to bond with its adjacent atom (N atom in AlNC and C atom in AlCN) are 0.154 and 0.123 at the B3LYP level, 0.134 and 0.104 by MP2 calculations, and 0.129 and 0.092 with the QCISD method in AlNC and AlCN molecules, respectively. The CN distance is longer and the bond order (Al atom to its adjacent C or N atom) is larger in AlNC than in AlCN; thus, the AlNC isomer should be more stable than the AlCN structure. This is proved by the energy difference mentioned above for the two molecules.

The transition state between linear AlNC and AlCN was determined by B3LYP and MP2 methods. It is a triangular structure, with 2.110 (B3LYP) and 2.091 (MP2) Å for bond Al−C and 2.293 (B3LYP) and 2.250 (MP2) Å for Al−N, respectively. The activation energies of 12.75 (B3LYP) and 8.64 (MP2) kcal/mol are needed to isomerize from AlNC to AlCN. According to the results of Schaefer et al.,[14] AlNC is the more stable isomer by 5.5 kcal/mol and there is a 6 kcal/mol activation energy for the isomerization of AlCN to AlNC. The difference in energy between AlNC and AlCN is 6.09 (B3LYP), 1.19 (MP2), and 4.04 (QCISD(T)) kcal/mol. The activation energies of 7.45 (MP2) and 6.68 (B3LYP) were obtained for the isomerization from AlCN to AlNC. Our B3LYP calculations are more compatible with those of ref 8 than those of the MP2 method.

The calculated lowest frequencies of the two molecules are 146.7 (B3LYP), 156.8 (MP2), and 168.1 (QCISD) cm^{-1} for the AlCN isomer and are 102.8 (B3LYP), 100.8 (MP2), and 116.0 (QCISD) cm^{-1} for AlNC, all with π symmetry. The only imaginary frequency of the transition state is i209.2 (B3LYP) and i191.5 (MP2) cm^{-1}. Calculations of frequencies and isomerization of these isomers are presented in Table 5 and Figure 3, respectively.

We also calculated related HCN and HNC molecules with the same methods. Since the H atom is substituted by an Al atom in HCN or HNC, the bond length of C−N or N−C is lengthened. For example, in HNC, the NC distance is 1.169 (B3LYP) and 1.181 (MP2) Å, while it is 1.181 (B3LYP) and 1.193 (MP2) Å in AlNC. This may be because the large core charge of the Al atom disperses the electron cloud between C and N atoms.

3.4. AlC_2N. Optimizations were performed on several possible isomers of the AlC_2N molecule, and we got several linear and nonlinear stationary points on the potential surface, all with planar structures. With both B3LYP and MP2 methods, the C_s form (nonisosceles triangle composed of Al, C, and N atoms, with the other C atom located in the middle; see also Figure 1) was calculated to be much more stable in energy than the other six forms. The relative energies of the seven structures are presented in Table 1. A similar form C_{2v} (with the N atom inside the isosceles triangle composed Al and two C atoms) was calculated to be a first-order saddle point, with imaginary

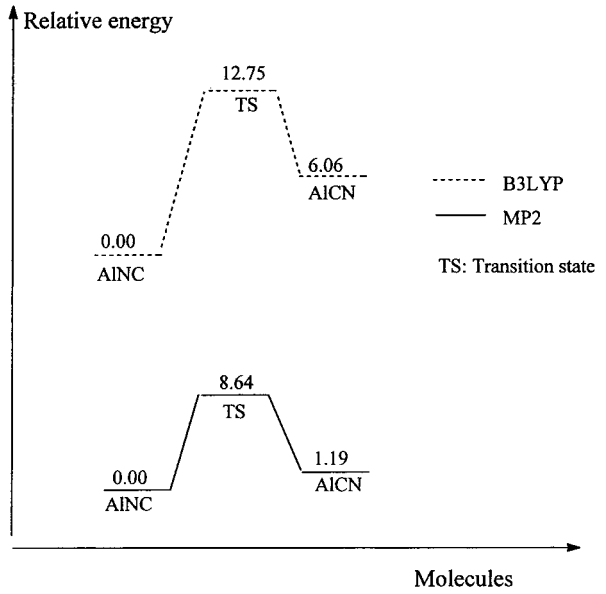

Figure 3. Relative energies of AlNC and AlCN and activation energy of the isomerization between them at B3LYP and MP2 levels.

frequencies of i510.3 and i521.5 with b_2 symmetry at the two levels. Its energy is 51.78 (B3LYP) and 54.53 (MP2) kcal/mol higher than the energy of the C_s form. For the ground state of the AlC_2N (C_s) molecule, its electronic state is predicted to be $^1A'$.

For the AlC_2N (C_s) isomer, its calculated frequencies at the two levels are listed in Table 5. For the other six true minima from **II** to **VII** (see also Figure 1), their lowest fundamental frequencies are as follows: 215.7 (π), 170.5 (b_1), 180.8 (π), 225.1 (π), 157.0 (π), and 137.2 (π) cm^{-1} by B3LYP calculation, and 187.9 (π), 185.4 (b_1), 210.0 (π), 192.0 (π), 154.7 (π), and 126.7 (π) cm^{-1} at the MP2 level. Values for the same isomer at the two levels agree with each other primarily.

To estimate the thermodynamic stabilities of AlC_2, AlC_3, AlNC, and AlC_2N molecules, additional calculations were done for dissociations into Al and C_2, C_3, and C_2N species. For the C_3 species, both D_{3h} and linear $D_{\infty h}$ structures were calculated at both singlet and triplet states. The $D_{\infty h}$ (singlet) structure was predicted to be the global minimum, and its energy was calculated to be 48.69 (B3LYP) and 45.82 (MP2) kcal/mol lower than the $D_{\infty h}$ (triplet) one. For example, at B3LYP level, the dissociation energies of the following reactions

$$AlC_2\ (C_{2v}) \rightarrow Al + C_2 \quad (1)$$

$$AlC_3\ (C_{2v}) \rightarrow Al + C_3(D_{\infty h}) \quad (2)$$

$$AlC_2N\ (C_s) \rightarrow Al + C_2N\ (C_{2v}) \quad (3)$$

are 144.52, 35.39, and 76.23 kcal/mol, respectively. At the MP2 level, the values are 150.66, 40.26, and 53.76 kcal/mol instead. Computational results of the above and other related dissociation reactions at both B3LYP and MP2 levels are provided in Table 2. From these data, the great thermodynamic stabilities of these aluminum carbides, cyanides, and isocyanides that we considered are obvious.

4. Conclusion

From above-mentioned results and discussion, we summary our investigations as follows.

1. Optimizations were performed on the AlC_n ($n = 2, 3$) and AlC_nN ($n = 1, 2$) series. The most stable structure of AlC_2 was predicted to be in an isosceles triangle (C_{2v}) form at the doublet state, and that of AlC_3 was calculated to be a deformed rhombus at the quadruplet state. The global minimum of AlC_2N was confirmed to adopt C_s configuration at both levels, and singlet states are all adopted as the ground states for AlCN, AlNC, and AlC_2N molecules.

2. Transition states and IRC calculations were performed for AlC_2 and AlNC at B3LYP and MP2 levels. Transition states for AlC_2 and AlNC adopt obtuse and acute triangular configurations successively, and they connect the two stable isomers of the AlC_2 and AlNC molecules through IRC investigations.

3. The relative energy of the linear $C_{\infty v}$ isomer for the AlC_2 molecule is 8.77, 21.39, and 11.39 kcal/mol higher than that of C_{2v} isomer at B3LYP, MP2, and QCISD(T) levels, respectively. The AlNC isomer is 6.09, 1.19, and 4.04 kcal/mol lower in energy than the AlCN isomer at the three levels. Our calculated values at B3LYP and QCISD(T) levels coincide with those from refs 10 and 13 and ref 8 quite well.

4. These global minima are predicted to be thermodynamically stable toward dissociation, and all possible dissociation reactions were calculated to be greatly endothermic. It is probable that these molecules will be found in interstellar space.

5. The predicted vibrational frequencies at the three levels coincide with one another very well, and they may be useful for analysis of unidentified lines in laboratory experiments.

Acknowledgment. We are grateful to National Science Foundation of China for financial support.

References and Notes

(1) Kawaguchi, K.; Ohishi, M. Personal communication, 1995.

(2) Guelin, M.; Cernicharo, J.; Kahane, C.; Gomez-Gonzalez. *J. Astron. Astrophys.* **1986**, *157*, L17.

(3) Kieninger, M.; Irving, K.; et al. *J. Mol. Struct.: THEOCHEM* **1998**, *422*, 133.

(4) Kawaguchi, K.; Kagi, E.; Hirano, T.; Takano, S.; Saito, S. *Astrophys. J.* **1993**, *406*, L39.

(5) Ishii, K.; Hirano, T.; Nagashima, U.; Weis, B.; Yamashita, K. *Astrophys. J.* **1993**, *410*, L43.

(6) Green, S. *Chem. Phys. Lett.* **1984**, *112*, 29.

(7) Bauschlicher, C. W., Jr.; Langhoff, S. R.; Partridge, H. *Chem. Phys. Lett.* **1993**, *216*, 341.

(8) Da Silva, C. O.; Da Silva, E. C.; et al. *Int. J. Quantum Chem.* **1995**, *29*, 639.

(9) Alexander, I. B.; Jack, S. *J. Phys. Chem. A* **1997**, *101*, 2215.

(10) Yang, H. L.; Tanaka, K; Ahinada, M. *J. Mol. Struct.: THEOCHEM* **1998**, *422*, 159.

(11) Flores, J. R.; Largo, A. *Chem. Phys.* **1990**, *140*, 19.

(12) Knight, L. B., Jr.; Cobranchi, S. T.; Herlong, J. O.; Arrington, C. A. *J. Chem. Phys.* **1990**, *92*, 5856.

(13) Chertihin, G. V.; Andrews, L.; Taylor, P. R. *J. Am. Chem. Soc.* **1994**, *116*, 3513.

(14) Ma, B.; Yamaguchi, Y.; Schaefer, H. F. *Mol. Phys.* **1995**, *86*, 1331.

(15) Lanzisera, D. V.; Andrews, L. *J. Phys. Chem. A* **1997**, *101*, 9660.

(16) Solegel, H. B. *J. Comput. Chem.* **1982**, *3*, 214.

(17) Hehre, W. J.; Random, L.; Schleyer, P. v. R.; Pople, J. A. *Ab Initio Molecular Orbital Theory*; Wiley: New York, 1986.

(18) Lee, C.; Yang, W.; Parr, R. G. *Phys. Rev. B* **1988**, *37*, 785. Beche, A. D. *Phys. Rev. A* **1988**, *38*, 3098.

(19) Pople, J. A.; Head-Gordon, M.; Raghvachari, K. *J. Chem. Phys.* **1987**, *87*, 5968.

(20) Gonzalez, C.; Schlegel, H. B. *J. Chem. Phys.* **1989**, *909*, 2154.

(21) Gonzalez, C.; Schlegel, H. B. *J. Phys. Chem.* **1990**, *94*, 5523.

(22) Frisch, M. J.; Trucks, G. N.; Schlegel, H. B.; Pople, J. A.; et al. *Gaussian 94*, revision E.2; Gaussian Inc.: Pittsburgh, PA, 1995.

(23) Zheng, X.; Wang, Z.; Tang, A. *J. Mol. Struct.: THEOCHEM*, in press.